## Title

Lithium substituted poly(amic acid) as a water-soluble anode binder for high-temperature pre-lithiation



## Authors

Zhu, Tianyu
Tran, Thanh-Nhan
Fang, Chen
et al.

## Publication Date

2022-02-01

## DOI

10.1016/j.jpowsour.2021.230889

Peer reviewed

Journal of Power Sources 521 (2022) 230889

Contents lists available at ScienceDirect

Journal of Power Sources

journal homepage: www.elsevier.com/locate/jpowsour

# Lithium substituted poly(amic acid) as a water-soluble anode binder for high-temperature pre-lithiation

Tianyu Zhu [a], Thanh-Nhan Tran [a], Chen Fang [a], Dongye Liu [b], Subramanya P. Herle [c], Jie Guan [c], Girish Gopal [c], Ajey Joshi [c], James Cushing [c], Andrew M. Minor [b], Gao Liu [a,*]

[a] Energy Storage & Distributed Resources Division, Lawrence Berkeley National Laboratory, Berkeley, CA, 94720, United States
[b] Department of Materials Science and Engineering, University of California, Berkeley, National Center for Electron Microscopy, Molecular Foundry, Lawrence Berkeley National Laboratory, Berkeley, CA, 94720, United States
[c] Applied Materials, Inc, Santa Clara, CA, 95054, United States

## HIGHLIGHTS

- A water-soluble lithium substituted poly (amic acid) binder was designed for Si electrodes.
- Thermal imidization of lithium substituted poly(amic acid) to polyimide was achieved.
- Polyimide binder based Si electrodes are thermally stable up to 500 °C.
- High temperature pre-lithiation can be performed on these electrodes.

## GRAPHICAL ABSTRACT

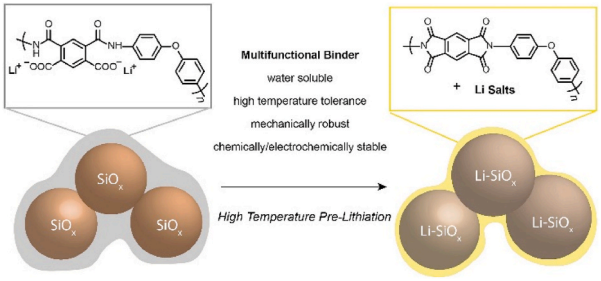


## ABSTRACT

Multifunctional binders hold great promise in advanced electrode designs for both fundamental research and practical utilization of lithium-ion batteries (LIBs). The reactions between Si/$SiO_x$-dominated anodes with lithium are expected to be exothermic in principle, while the thermal tolerance along with the volume change makes high-temperature binders attractive for large scale roll-to-roll manufacturing. For instance, if a high temperature binder is also water soluble, it can be compatible with the current graphite-based anode manufacturing process. In this work, we present a water-soluble poly(amic acid)-based binder, which can withstand high temperature for industrial pre-lithiation process and effectively hold active materials together during repeated charge and discharge cycles. This lithium substituted poly(amic acid) binder (denoted as Li-Pa) can serve as a drop-in replacement for environmentally friendly electrode fabrication in large scale by providing aqueous solubility, exceptional thermal stability and mechanical flexibility.

## 1. Introduction

Secondary energy storage devices based on lithium-ion transport have gained increasing interest for their light weight, high energy density and outstanding charge-discharge capabilities [1,2]. Among various anode materials, carbon-based anodes have been extensively explored and widely utilized for their high electrochemical reversibility, but largely limited by their low capacity (372 mAh/g for graphite). Compared with intercalation-type graphite anodes, alloy anodes provide considerably higher capacity (>3500 mAh/g for Si, 990 mAh/g for Sn), while suffering from substantial volume changes (~300% volume expansion from Si to $Li_{22}Si_4$, ~250% from Sn to $Li_{22}Sn_5$) as well as

* Corresponding author.
*E-mail address:* gliu@lbl.gov (G. Liu).

https://doi.org/10.1016/j.jpowsour.2021.230889
Received 29 September 2021; Received in revised form 11 November 2021; Accepted 6 December 2021
Available online 21 December 2021

severe interfacial side-reactions that continuously consuming electrolytes [3–5]. Downsizing the active particles (to nanoscale) and surface engineering of active materials have been demonstrated as effective approaches to tolerating volume change, avoiding pulverization, and thus enhancing the cycling life and capacity retention [6–10]. Besides, applying multifunctional polymer binders in anode fabrication represents another cost-effective method for practical applications. Especially, multifunctional binders with ideal physical properties can be employed with industrial available micro-sized particles, which are more attractive for their low cost and high tap density [11–13].

Over the past decades, a range of natural-based or synthetic polymers have been developed as electrode binders for LIBs, such as polyvinylidene fluoride (PVDF), polyacrylic acid (PAA), carboxymethyl cellulose/styrene-butadiene rubber (CMC-SBR) (Fig. 1a), polyethylene oxide (PEO), polyvinyl alcohol (PVA), polyfluorene-based conductive polymers, to name just a few [14–16]. The chemical properties of these binders, including their stability, mechanical properties, adhesion and cohesion behaviors greatly impact the manufacturing and cycling of the composite anodes (Table S1). Polyimide represents a class of synthetic polymers developed since 1900s, and shows outstanding mechanical property, thermal stability, and adhesive properties [17–19]. Derivatives of polyimide have recently been explored as effective binders for anodes and cathodes in reducing particle disintegration and accommodating the physical stress [20–25]. However, a major weakness for polyimide derivatives is their solubility [26]. The processing of polyimide derivatives is mostly based on organic solvents (*e.g.*, dimethylformamide or toxic chloroform), which is unfavorable for large scale and eco-friendly manufacturing process in battery industries.

In the meantime, LIB industry is looking into a large-scale process for the pre-lithiation, and direct roll-to-roll lithium deposition on the anode is gaining momentum. When the lithium is deposited on to the anode under inert or vacuum conditions, dry-contact pre-lithiation is initiated. Depending on the loading of Si/$SiO_x$ and porosity, lithium diffusion into the bulk of the electrode takes place over certain timescale and there will be volume changes associated with this process. For example, PAA binder was applied for Si anode (15.6 wt%) and vacuum based pre-lithiation showed longer cycling performance compared to non-pre-lithiated anode control [27]. These results clearly show a promising path for water processable binder with simple vacuum based pre-lithiation process for high volume manufacturing of advanced Si anode in the lithium-ion battery.

Herein, we present a water-soluble polymer, lithium substituted poly (amic acid) (denoted as Li-Pa), which can serve as a multifunctional anode binder and an important precursor to highly stable polyimide. Additionally, this binders can accommodate large-scale manufacturing process that requires high thermal stability and mechanical flexibility. The electrochemical performance was further evaluated in coin cell study with commercial $SiO_x$ (micro-sized) as active materials, together with an industrial high temperature pre-lithiation process.

## 2. Experimental section

***Materials.*** Poly(pyromellitic dianhydride-*co*-4,4′-oxydianiline) amic acid solution (~15 wt%) in *N*-methyl-2-pyrrolidone (NMP), lithium hydroxide (>98%) were purchased from Sigma-Aldrich and used as received. $SiO_x$ active material was obtained from Shinetsu and used as received. Graphite for electrode fabrication was purchased from Hitachi. Lithium iron phosphate ($LiFePO_4$, LFP) cathode, Generation second lithium-ion electrolyte (1.2 M $LiPF_6$ in ethylene carbonate, ethyl methyl carbonate (EC/EMC = 3/7 w/w)) were obtained from Argonne National Laboratory and directly used in cell assembly. Celgard 2400 separator was purchased from Celgard.

***Synthesis of Li-Pa binder.*** Poly(amic acid) (**1**) was obtained by slow precipitation of a commercial solution (15 wt% in NMP) in deionized (DI) water, further collected by filtration and dried at 50 °C under vacuum to remove remaining solvents. In an aqueous solution of lithium hydroxide (same equivalent to the calculated carboxylic acid groups), polyamic acid polymer (yellow fiber, insoluble in water) were added, followed by continuous stirring overnight. After the reaction, Li-Pa (**2**) was completely dissolved in the water, forming a viscous solution (5 wt %) which can be directly applied for electrode fabrication, while the pure polymer of lithium polyamic can be obtained by freeze-drying the aqueous solution as white fluffy fibers. $^1$H NMR of Li-Pa (500 MHz, $D_2O$): δ = 7.15 (*s, phenol ether alpha proton*, 4H), 7.53 (*s, phenol ether beta hydrogen*, 4H), 7.92, 7.83, 7.75 (*s, acetate substituted phenol*, 2H).

***Thermal imidization of Li-Pa.*** Generally, polyimide (**3**) was synthesized by thermal imidization of Li-Pa (**2**). Imidization was achieved by heating the polyamic precursor (in the form of polymer fiber, or thin

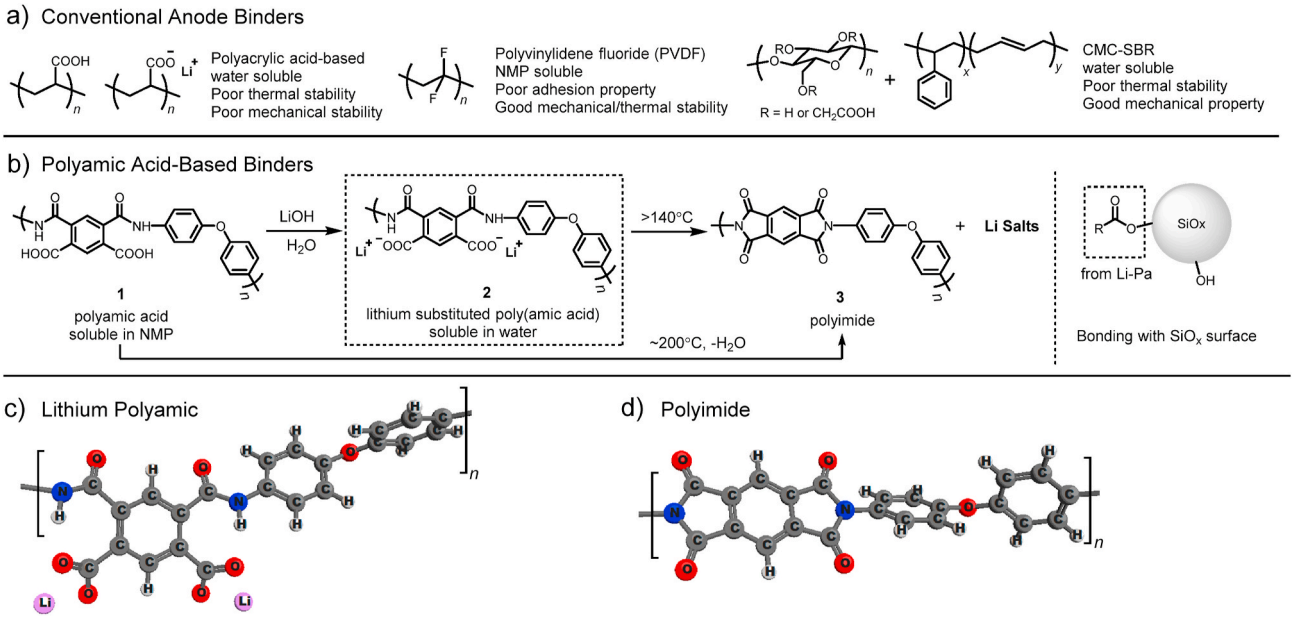


**Fig. 1. (a)** Chemical structures and properties of conventional polyacrylic-based, polyvinylidene fluoride and CMC-SBR binders; **(b)** Synthesis of water-soluble poly (amic acid)-based binder, its thermal conversion to corresponding polyimide, and covalent bonding with $SiO_x$ materials; Optimized molecular structures for **(c)** Li-Pa and **(d)** conventional polyimide.

film, or electrode binder) to >140 °C for a certain time. The resulting polyimide is insoluble in most organic solvents and water.

***Electrode fabrication.*** 1) $SiO_x$ anodes with various binders. In a homogeneous solution of Li-Pa binder in DI water (5 wt%), $SiO_x$ (active material), graphite and Denka black were sequentially added and thoroughly mixed under room temperature. Similarly, the solvent used for polyacrylic-based binder is DI water, while NMP was used to dissolve PVDF binder. The weight ratios of binder, $SiO_x$, graphite and Denka black are 15%, 60%, 20% and 5%, respectively. The slurry was coated on a copper foil using a doctor blade and dried at 80 °C in a vacuum oven. The resulting anode has an areal capacity of ~1.6 mAh/cm$^2$ for half cells and ~2.5 mAh/cm$^2$ for full cells (corresponding to 1.1 $mg_{SiOx}$/cm$^2$ and 1.7 $mg_{SiOx}$/cm$^2$, respectively) to match practical needs. 2) Binder electrodes (used in cyclic voltammetry tests to understand the chemical and electrochemical stability of polymer binder towards lithiation/delithiation). In a homogeneous solution of Li-Pa in DI water (5 wt%), Denka black (to ensure good conductivity) was added and thoroughly mixed with the binder solution. The weight ratios of polymer, Denka black are 70% and 30% respectively. The slurry was coated on a copper foil using a doctor blade and the coated electrode was dried at 80 °C in the vacuum oven.

***Coin cell fabrication.*** Coin cell (CR2032, MTI Corp.) assembly was performed in an argon-filled glovebox. A 14.42 mm diameter disk was punched out as a working electrode. Lithium chip (16.0 mm in diameter, MTI Corp.) or LFP cathode was used as the counter electrode. 60 μL of 1.2 M $LiPF_6$ in EC/EMC = 3/7 electrolyte (Generation 2, obtained from Argonne National Lab) with (or without) fluoroethylene carbonate (FEC, 5 wt%) was used for various electrochemical tests. Celgard 2400 separator (1.7 cm in diameter) was placed between the working electrode and the counter electrode.

***Coin cell tests.*** Cycling performance of the assembled coin cells was evaluated in a thermal chamber at 30 °C with a Maccor Series 4000 Battery Test System. The cut-off voltages for cell testing are 0.01–1.0 V for half cells ($SiO_x$/Li), and 2.5–4.0 V for full cells ($SiO_x$/LFP), assuming a theoretical capacity of 1,200 mAh/g for $SiO_x$. In galvanostatically cycling tests, the half cells were cycled at a rate of C/10, while the full cells were pre-cycled at a rate of C/25 for three cycles, then at a rate of C/10. The C rate here was determined by the theoretical capacity of $SiO_x$. The specific capacity of the composite anode material was reported based on the amount of $SiO_x$ considering the carbon additives contribute to less than 10% of overall capacity. The full cell impedance was measured on a VSP300 potentiostat (Biologic Co.) with frequency range was from 100 mHz to 1 MHz under AC stimulus with 10 mV of amplitude and no applied voltage bias. The cell was charged to 3.20 V and held for 4h before the impedance measurement.

***Anode Pre-lithiation.*** Anode pre-lithiation was realized by high temperature vapor deposition of Li at Applied Materials with an industrial sheet-to-sheet process. The amount of deposited lithium was controlled to cover the first cycle loss based on results from the half cell testing.

***Mechanical tests.*** *For polymers*: the hardness and elastic modulus of bulk polymers with a thickness of 15 μm were analyzed with Hysitron TI 950 TriboIndenter nanoindenter. A conical sphere 10 μm probe was used and calibrated with polycarbonate as standard. The peak load for indentation measurements was 9000 μN with a load rate of 300 nm/s. *For electrodes*: Typically, an electrode strap with a size of 1 × 3 cm was used for the bending tests. The electrode strap was curved to 4.8 mm in diameter and the morphology of the bent area was further observed under scanning electron microscopy (SEM).

***Other characterizations.*** $^1$H NMR (500 MHz) spectra were recorded on a Bruker Avance II 500 MHz NMR Spectrometer (Molecular Foundry at Berkeley Lab) using deuterated oxide ($D_2O$) as the solvent and all chemical shifts were compared to deuterated solvents or tetramethylsilane (TMS) as a reference. The surface images of composite anodes were collected with SEM (JSM-7500F JOEL, Japan) under high vacuum and an accelerating voltage of 12 kV. Fourier-transform infrared spectroscopy (FT-IR) of polymer samples was recorded on Nicolet iS50 FTIR with attenuated total reflectance (ATR) function. The surface area was measured by the Brunauer Emmett Teller (BET) $N_2$ adsorption method using TriStar II Plus (Micrometrics, USA). Differential scanning calorimetry (DSC) and thermogravimetric analysis (TGA) of polymer binders were conducted with thermal analyzer from TA Instruments (USA). X-ray diffraction of polymers and active materials were recorded on a Bruker D2 phaser benchtop X-ray diffractometer system. Transmission electron microscope (TEM) images were obtained on a FEI monochromated F20 UT Tecnai microscope operated under 200 kV at the National Center for Electron Microscopy (NCEM).

## 3. Results and discussion

There is an emerging trend in polymer binder design to accommodate manufacturing needs and support durable cell cycling. We first considered the solubility of anode binders, as both research community and battery manufacturing industry continue to proceed toward environmentally benign processes by phasing out or recycling organic solvents in electrode fabrication. With regard to polyimide, the rigidity of aromatic backbone usually results in challenges to dissolve or melt the polymer at low temperature [26]. For example, Kapton, a commonly known product of polyimide, can only be processed in its precursor form of poly(amic acid). Thus, we conceptualized to use a water-soluble poly (amic acid)-based precursor, which can be thermally converted to highly stable polyimide. Ideally, the thermal imidization reaction for this precursor can be carried out at a relatively lower temperature (<200 °C) while without generating water as a byproduct considering water can react with lithium ($2H_2O+2Li = 2LiOH + H_2$) and weaken the adhesion. For poly(amic acid), abundant carboxylic acid groups (-COOH) in the backbones provide significant intra- and intermolecular interactions. Herein, carboxylic acid groups were converted to acetate groups ($-COO^-$) using LiOH to weaken the intermolecular interactions and enhance the water solubility (Fig. 1b). The optimized molecular structures of Li-Pa and polyimide were illustrated in Fig. 1c and d, and the chemical structure of Li-Pa was further evidence by $^1$H NMR in $D_2O$ (Fig. 2a). In addition, a lithium salt instead of water molecule will be produced during the thermal imidization, which satisfies the high temperature pre-lithiation requirements. As shown in Fig. 2b and c, DSC was used to probe imidization of Li-Pa in comparison to poly(amic acid). A lower onset temperature for the endothermal reaction was observed for Li-Pa (first heating curve, ~140 °C) due to the stronger nucleophilicity of acetate groups, which makes the thermal imidization kinetically favored. Furthermore, there was no endo-/exothermic peak witnessed in the second heating process for both polymers, indicating a complete imidization during the first heating process and high thermal stability of the products.

In the development of tailored polymer binders, reactive functional groups such as -OH, -COOH, and $-NH_2$, which are capable of forming strong hydrogen bonds, ion-dipole interactions, and covalent chemical bonds that are far stronger than van der Waals forces, play a crucial role [28,29]. For low loading cases, CMC-SBR binder has provided some promising results for both Si- and $SiO_x$-based anodes. The search for suitable water processible binders was further extended in the literature towards other polymers such as PAA, PVA and alginate [30]. Furthermore, binders with abundant polarizable moieties bestow moderately strong but elastic interactions with additional self-healing or reversible properties. For Li-Pa binder, rich acetate groups on the polymer matrix can covalently bond to the surface of $SiO_x$ through the *trans*--esterification reaction during the electrode drying process [31]. In-depth understanding on the structure-property correlations (including bonding type, bonding strength) could further elucidate the working mechanisms of these binders in Si/$SiO_x$ anode cells [32]. The chemical structures of poly(amic acid), Li-Pa and their imidization products were further analyzed by FT-IR (Fig. 2d). These polymers share some characteristic peaks located at 820 cm$^{-1}$, 1013 cm$^{-1}$, 1229 cm$^{-1}$, 1493 cm$^{-1}$

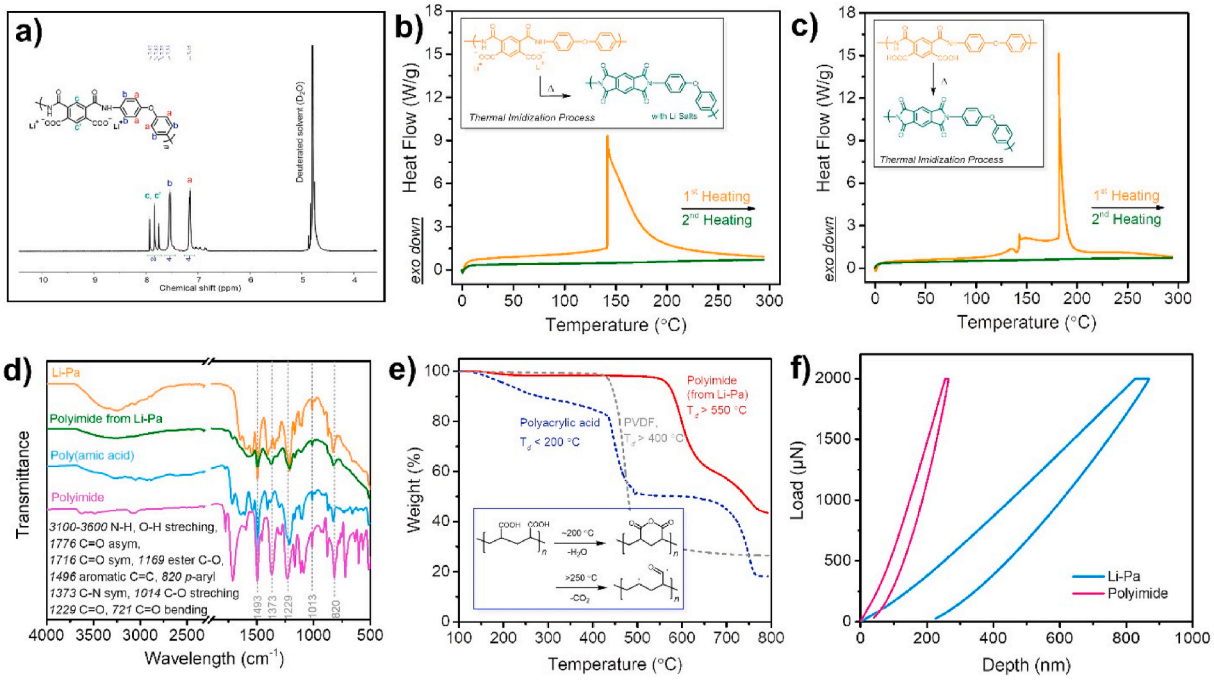


**Fig. 2.** **(a)** $^{1}$H NMR spectrum of Li-Pa binder in the deuterated water. We noted that conventional poly(amic acid) polymer is insoluble in aqueous solvents; DSC curves of the first and second heating processes for **(b)** Li-Pa and **(c)** polyamic acid at a ramping rate of 30 °C/min, insets: reaction scheme for thermal imidization; **(d)** FT-IR spectral comparison for poly(amic acid), Li-Pa and their imidization products; **(e)** TGA profiles of polyacrylic acid, polyvinylidene fluoride and polyimide (prepared by thermal imidization of Li-Pa), inset: thermal degradation pathway for polyacrylic acid; **(f)** Load-depth profile for Li-Pa and conventional polyimide in nanoindentation measurements.

corresponding to *p*-aryl, C-O, C=O and aromatic C=C functionalities, respectively. Li-Pa also exhibits a broad absorption band in the range of 3100–3600 $cm^{-1}$ resulted from strong N-H and O-H stretching. Besides, the disappearance of peak at ~1650 $cm^{-1}$, which is attributed to the specific amide C=O stretching in poly(amic acid)-based precursor, suggests a complete imidization to form polyimide [33].

Many of conventional binders are either mechanically weak or thermally unstable, which limit their compatibility with new manufacturing processes. For example, polyacrylic acid and its derivatives are frequently used as anode binder for silicon-based anodes. However, their thermal decomposition temperature is low. For instance, dehydration from the carboxylic acid groups (in polyacrylic acid) happens at ~200 °C, and decarboxylation occurs at ~250 °C (Fig. 2e). Further chain scission happens at a higher temperature causing poor mechanical and electrochemical properties. Besides, water is formed during the thermal degradation of polyacrylic acid, which it is unfavorable in the pre-lithiation process. On the other hand, polyimide materials are known to be resistant to heat and chemicals. The synthesized lithium polyimide shows excellent thermal stability without obvious thermal degradation below 550 °C. Such thermal stability is ideal for its application as a binder for high temperature pre-lithiation process.

Apart from consideration of thermal stability, mechanical property is essential especially for large scale roll-to-roll production. We first evaluated the bulk mechanical properties of Li-Pa and polyimide in comparison to few commodity polymers (Figs. 2f and S1) through nanoindentation. Poly(amic acid)-based polymers (Li-Pa and polyimide) provide significantly higher hardness (0.27–0.50 GPa) compared to PVDF (<0.1 GPa), largely due to more rigid polymer backbones. On the other hand, the elastic modulus of Li-Pa (1.6 GPa) is lower than poly (amic acid)-based polymer (6.2 GPa) because the intermolecular interaction (including hydrogen bonding) has been weakened by the incorporation of lithium salts. Moreover, at the electrode level, polyacrylics are known to become extremely brittle upon drying (<50 ppm), which limits their industrial application. In comparison, polyimide coating was expected to homogeneously cover the surface for all the particles and provide improved elasticity to composite anodes. Indeed, no polymer aggregate was observed in the SEM image of the composite anodes, indicting the excellent surface coating behavior of Li-Pa (Fig. S2). TEM images further reveal that the Li-Pa binder forms a uniform ~25 nm coating layer on the active particles (Fig. S3). XRD pattern of the polymer thin film also confirms its amorphous microstructure, which is similar to conventional polyimide (Fig. S4). SEM was also applied to monitor the pristine state and any crack formation under mechanical bending (Fig. 3a,e). No crack was observed for $SiO_x$ anodes with Li-Pa binder, which indicates the superior mechanical flexibility and binding property of poly(amic acid)-based polymers (Fig. 3b,f). In comparison, polyacrylics exhibit low toughness and are easily broken when bent to cylindrical form. For composite electrode with polyacrylic binder, obvious cracks were formed form during drying and bending the electrodes due to the strong interaction of carboxylic acid groups with water as well as the mechanical brittleness of polyacrylics (Fig. 3c,g).

Considering the electrochemical stability and cycling efficiency, graphite has been mostly utilized as an anode material in LIBs compared to other alloy materials. Graphite anode fabricated with lithium Li-Pa binder also delivered exceptional cycling stability and high Coulombic efficiency (Fig. S5), benefiting from the exceptional stability of binder towards lithiation/delithiation. Although PAA and PVDF also function well for carbon-based materials, they usually underperform for silicon-based anodes. For instance, PVDF is easily weakened, losing the mechanical strength to hold active materials together during cycling. In order to mitigate the impact of various active materials, electrochemical performance of composite anodes fabricated with an industrial $SiO_x$ materials and different binders (PAA, PVDF, Li-Pa) were evaluated. Fig. S6 shows the SEM image of pristine $SiO_x$ with a size of approximately <10 μm. X-Ray diffraction (XRD) of the active materials revealed characteristic peaks from $SiO_x$ (Fig. 3d) and the BET surface area of $SiO_x$ was measured to be 3.20 $m^2/g$ (Fig. S7).

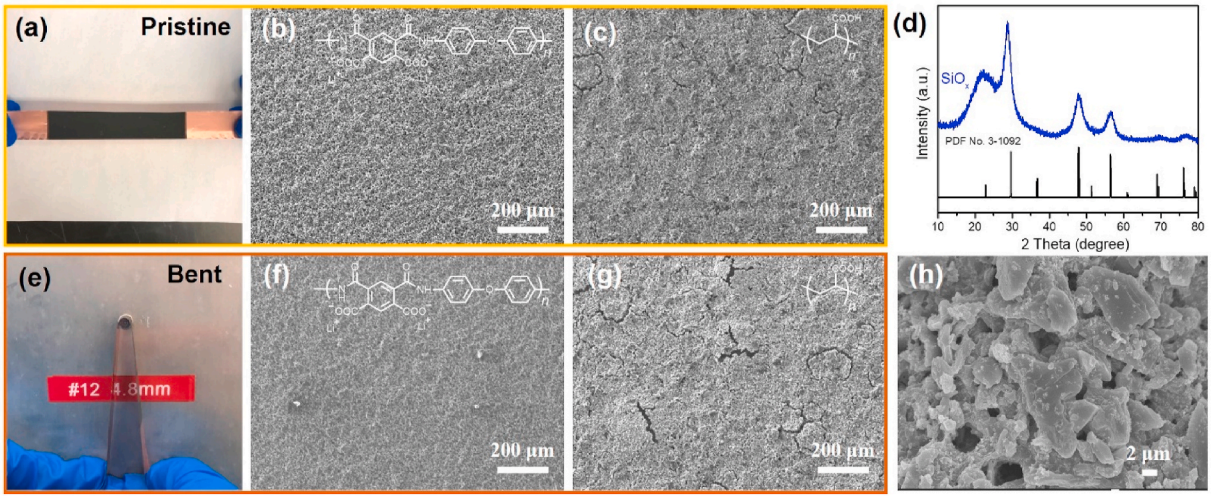


**Fig. 3.** **(a)** Pristine composite anode for mechanical bending tests; SEM images for pristine anodes with **(b)** Li-Pa and **(c)** polyacrylic acid binder; **(d)** XRD pattern for the industrial $SiO_x$ active material; **(e)** Image of a composite anode at bent state; SEM images of composite anodes with **(f)** Li-Pa and **(g)** polyacrylic acid binder after bending tests; **(h)** enlarged SEM images of composite anodes with Li-Pa binder.

The electrochemical stability of Li-Pa and polyimide were first evaluated using cyclic voltammetry as shown in Fig. S8. At the first cathodic scan, the characteristic peaks which indexed to the electrolyte decomposition can be observed. In the following cycles, both binders show no obvious redox peaks within the typical anode cycling window, indicating their superior electrochemical stability. Fig. 4a compares the cycling performance of $SiO_x$ anodes with various binders in half cells at a cycling rate of C/10. The Coulombic efficiencies were also summarized in Table S2. It is worth noting that a higher Coulombic efficiency would benefit the cycling stability and lifespan in a practical full battery. The initial charge capacities turned out to be similar, 1435 mAh/g (PVDF), 1466 mAh/g (Li-Pa) and 1411 mAh/g (lithium polyacrylic), suggesting $SiO_x$ anodes with different binders have similar reaction kinetics in the initial cycles. However, $SiO_x$ anode with PVDF binder suffers a rapid capacity fading, and the cell was terminated within 20 cycles. Such fast performance decay arises from poor adhesion and mechanical properties of PVDF, which can barely withhold the repeated volume changes of silicon-based anodes during lithiation/delithiation. In drastic contrast, polyacrylic and poly(amic acid)-based binders result in extended cycling lifespan and stability, delivering a capacity retention of 56% and 87% after 50 cycles, respectively. These results also agree well with the mechanical properties, especially the hardness of bulk polymers. Moreover,

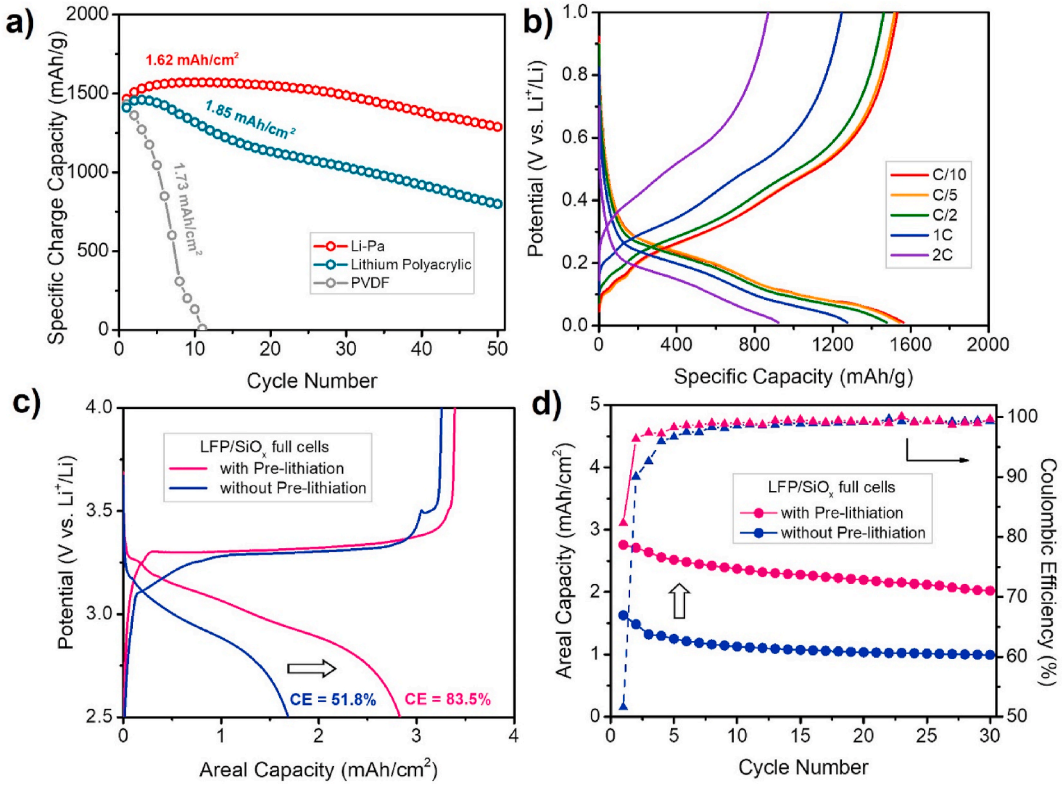


**Fig. 4.** **(a)** Cycling performance of $SiO_x$ anodes with various binders at a rate of C/10 in half cells; **(b)** The rate performance of $SiO_x$ anodes with Li-Pa binder; **(c)** First cycle charge-discharge profiles, and **(d)** Cycling performance and Coulombic efficiency of $SiO_x$/LFP full cells with and without pre-lithiation.

$SiO_x$ anodes with Li-Pa binder deliver high reversible capacities of 922, 1278, 1482 mAh/g at current rates of 2C, 1C and C/2, respectively (Fig. 4b). Further cycling at a rate of C/3 delivered a capacity retention of 70% after 100 cycles (Fig. S10). This result is encouraging considering the high loading of micro-sized $SiO_x$ (60 wt%) and low amount of electrolyte additive (5% FEC). It can be deduced that Li-Pa may benefit for 1) its high modulus and elasticity, which can withstand the stress generated by the expansion of $SiO_x$ during lithiation, and 2) its great surface coating property, to suppress the interface reactions between $SiO_x$ surfaces and electrolyte.

Anode pre-lithiation has become an important strategy to compensate for lithium loss in LIBs [34–36]. To illustrate the practical utilization, full cells fabricated with LFP cathode and composite anode with Li-Pa binder were evaluated. High temperature pre-lithiation was also applied on the anode side to improve the energy density. Fig. 4c presents the initial charge-discharge profiles of full cells with (and without) anode pre-lithiation at a current density of 50 mA/g (formation cycles). Clearly, the pre-lithiation process can effectively compensate the first cycle Li loss, rendering an improved initial discharge capacity corresponds to a higher Coulombic efficiency for the pre-lithiated anodes (2.83 mAh/cm$^2$, 83.5%) when compared with pristine ones (1.68 mAh/cm$^2$, 51.8%). In addition, the average potential of the pre-lithiated LFP/$SiO_x$ cell is slightly higher than full cell without pre-lithiation, which also contributes to a higher energy density. Benefiting from the high thermal stability and mechanical robustness of Li-Pa binder, the resulting anodes can withstand high temperature without sacrificing cycling stability and the Coulombic efficiency reached >99% within eight cycles and maintained thereafter (Fig. 4d). An areal capacity of >2.0 mAh/cm$^2$ was retained after 30 cycles for prelithiated anodes in full cell cycling, while anodes without pre-lithiation delivered less than half capacity (<1.0 mAh/cm$^2$). Full cell performance of lithiated anode at a higher cycling rate was also provided in Fig. S12. To further validate the potential in actual applications, full cells with enhanced capacity retention (67.7% after 300 cycles) and cycling efficiency (~99.8% on average) were achieved by adjusting the active material loading and cycling conditions (Fig. S13).

## 4. Conclusions

In summary, we developed a water-soluble poly(amic acid)-based binder for $SiO_x$ anodes and high-temperature pre-lithiation. Composite anodes with Li-Pa binder outperform two signature commercial binders in half cell cycling, providing an 87% capacity retention after 50 cycles (70% capacity retention after 100 cycles). Given the superior thermal stability and mechanical flexibility of Li-Pa binder, the composite anodes can accommodate high-temperature manufacturing process to compensate irreversible Li loss during cycling, and as a result, full cells based on lithiated $SiO_x$ anodes exhibit an initial discharge capacity of 2.83 mAh/cm$^2$ and a Coulombic efficiency of 83.5%. For instance, understanding and utilization of such multifunctional binders as a drop-in replacement for conventional polyacrylic acid and PVDF will facilitate the development of commercial LIBs with high energy density towards large-scale manufacturing.

## Authors contribution

GL and TZ conceived and designed the experiments. TZ, TNT, CF and DL conducted the experiments. SPH, JG, GG, AJ, JC contributed to the designs of the experiments. AMM and GL supervised the research. TZ and GL wrote the manuscript with inputs from all authors.

## Declaration of competing interest

The authors declare that they have no known competing financial interests or personal relationships that could have appeared to influence the work reported in this paper.

## Acknowledgements

This research was funded by the Assistant Secretary for Energy Efficiency, Vehicle Technologies Office and Advanced Manufacturing Office of US Department of Energy, and Applied Materials, Inc. D.L. and A. M.M. were supported by the Toyota Research Institute. Lawrence Berkeley National Laboratory is supported by the Director, Office of Science, Office of Basic Energy Sciences, of the US Department of Energy under contract no. DE-AC02-05CH11231.

## Appendix A. Supplementary data

Supplementary data to this article can be found online at https://doi.org/10.1016/j.jpowsour.2021.230889.

## References

[1] M. Yoshio, R.J. Brodd, A. Kozawa, Lithium-ion Batteries, vol. 1, Springer, 2009.
[2] N. Nitta, F. Wu, J.T. Lee, G. Yushin, Li-ion battery materials: present and future, Mater. Today 18 (2015) 252–264.
[3] Y. Jin, B. Zhu, Z. Lu, N. Liu, J. Zhu, Challenges and recent progress in the development of Si anodes for lithium-ion battery, Adv. Energy Mater. 7 (2017), 1700715.
[4] W.-J. Zhang, A review of the electrochemical performance of alloy anodes for lithium-ion batteries, J. Power Sources 196 (2011) 13–24.
[5] H. Li, T. Yamaguchi, S. Matsumoto, H. Hoshikawa, T. Kumagai, N.L. Okamoto, T. Ichitsubo, Circumventing huge volume strain in alloy anodes of lithium batteries, Nat. Commun. 11 (2020) 1–8.
[6] C.K. Chan, H. Peng, G. Liu, K. McIlwrath, X.F. Zhang, R.A. Huggins, Y. Cui, High-performance lithium battery anodes using silicon nanowires, Nat. Nanotechnol. 3 (2008) 31–35.
[7] H. Wu, G. Yu, L. Pan, N. Liu, M.T. McDowell, Z. Bao, Y. Cui, Stable Li-ion battery anodes by in-situ polymerization of conducting hydrogel to conformally coat silicon nanoparticles, Nat. Commun. 4 (2013) 1–6.
[8] A. Zhang, Z. Fang, Y. Tang, Y. Zhou, P. Wu, G. Yu, Inorganic gel-derived metallic frameworks enabling high-performance silicon anodes, Nano Lett. 19 (2019) 6292–6298.
[9] A. Casimir, H. Zhang, O. Ogoke, J.C. Amine, J. Lu, G. Wu, Silicon-based anodes for lithium-ion batteries: effectiveness of materials synthesis and electrode preparation, Nano Energy 27 (2016) 359–376.
[10] X. Chen, X. Li, F. Ding, W. Xu, J. Xiao, Y. Cao, P. Meduri, J. Liu, G.L. Graff, J.-G. Zhang, Conductive rigid skeleton supported silicon as high-performance Li-ion battery anodes, Nano Lett. 12 (2012) 4124–4130.
[11] H. Chen, M. Ling, L. Hencz, H.Y. Ling, G. Li, Z. Lin, G. Liu, S. Zhang, Exploring chemical, mechanical, and electrical functionalities of binders for advanced energy-storage devices, Chem. Rev. 118 (2018) 8936–8982.
[12] F. Zou, A. Manthiram, A review of the design of advanced binders for high-performance batteries, Adv. Energy Mater. 10 (2020), 2002508.
[13] T. Chen, J. Wu, Q. Zhang, X. Su, Recent advancement of SiOx based anodes for lithium-ion batteries, J. Power Sources 363 (2017) 126–144.
[14] S. Li, Y.-M. Liu, Y.-C. Zhang, Y. Song, G.-K. Wang, Y.-X. Liu, Z.-G. Wu, B.-H. Zhong, Y.-J. Zhong, X.-D. Guo, A review of rational design and investigation of binders applied in silicon-based anodes for lithium-ion batteries, J. Power Sources 485 (2021), 229331.
[15] T. Zhu, G. Liu, Functional conductive polymer binder for practical Si-based electrodes, J. Electrochem. Soc. 168 (2021), 050533.
[16] D. Liu, Y. Zhao, R. Tan, L.-L. Tian, Y. Liu, H. Chen, F. Pan, Novel conductive binder for high-performance silicon anodes in lithium ion batteries, Nano Energy 36 (2017) 206–212.
[17] C. Feger, Advances in Polyimide: Science and Technology, CRC Press, 1993.
[18] H. Ohya, V. Kudryavsev, S.I. Semenova, Polyimide Membranes: Applications, Fabrications and Properties, CRC Press, 1997.
[19] D.-J. Liaw, K.-L. Wang, Y.-C. Huang, K.-R. Lee, J.-Y. Lai, C.-S. Ha, Advanced polyimide materials: syntheses, physical properties and applications, Prog. Polym. Sci. 37 (2012) 907–974.
[20] J.S. Kim, W. Choi, K.Y. Cho, D. Byun, J. Lim, J.K. Lee, Effect of polyimide binder on electrochemical characteristics of surface-modified silicon anode for lithium ion batteries, J. Power Sources 244 (2013) 521–526.
[21] S. Uchida, M. Mihashi, M. Yamagata, M. Ishikawa, Electrochemical properties of non-nano-silicon negative electrodes prepared with a polyimide binder, J. Power Sources 273 (2015) 118–122.
[22] J. Oh, D. Jin, K. Kim, D. Song, Y.M. Lee, M.-H. Ryou, Improving the cycling performance of lithium-ion battery Si/graphite anodes using a soluble polyimide binder, ACS Omega 2 (2017) 8438–8444.
[23] G. Qian, L. Wang, Y. Shang, X. He, S. Tang, M. Liu, T. Li, G. Zhang, J. Wang, Polyimide binder: a facile way to improve safety of lithium ion batteries, Electrochim. Acta 187 (2016) 113–118.
[24] B. Wilkes, Z. Brown, L. Krause, M. Triemert, M. Obrovac, The electrochemical behavior of polyimide binders in Li and Na cells, J. Electrochem. Soc. 163 (2015), A364.

[25] H.Q. Pham, G. Kim, H.M. Jung, S.W. Song, Fluorinated polyimide as a novel high-voltage binder for high-capacity cathode of lithium-ion batteries, Adv. Funct. Mater. 28 (2018), 1704690.
[26] A. Ghosh, S.K. Sen, S. Banerjee, B. Voit, Solubility improvements in aromatic polyimides by macromolecular engineering, RSC Adv. 2 (2012) 5900–5926.
[27] K. Kim, J. Shon, H. Jeong, H. Park, S.-J. Lim, J. Heo, Improving the cyclability of silicon anodes for lithium-ion batteries using a simple pre-lithiation method, J. Power Sources 459 (2020), 228066.
[28] T.-w. Kwon, J.W. Choi, A. Coskun, The emerging era of supramolecular polymeric binders in silicon anodes, Chem. Soc. Rev. 47 (2018) 2145–2164.
[29] T.-w. Kwon, J.W. Choi, A. Coskun, Prospect for supramolecular chemistry in high-energy-density rechargeable batteries, Joule 3 (2019) 662–682.
[30] J. Asenbauer, T. Eisenmann, M. Kuenzel, A. Kazzazi, Z. Chen, D. Bresser, The success story of graphite as a lithium-ion anode material–fundamentals, remaining challenges, and recent developments including silicon (oxide) composites, Sustain. Energy Fuels 4 (2020) 5387–5416.
[31] H. Zhao, Z. Wang, P. Lu, M. Jiang, F. Shi, X. Song, Z. Zheng, X. Zhou, Y. Fu, G. Abdelbast, Toward practical application of functional conductive polymer binder for a high-energy lithium-ion battery design, Nano Lett. 14 (2014) 6704–6710.
[32] G.G. Eshetu, H. Zhang, X. Judez, H. Adenusi, M. Armand, S. Passerini, E. Figgemeier, Production of high-energy Li-ion batteries comprising silicon-containing anodes and insertion-type cathodes, Nat. Commun. 12 (2021) 1–14.
[33] S. Kim, K.-S. Jang, H.-D. Choi, S.-H. Choi, S.-J. Kwon, I.-D. Kim, J.A. Lim, J.-M. Hong, Porous polyimide membranes prepared by wet phase inversion for use in low dielectric applications, Int. J. Mol. Sci. 14 (2013) 8698–8707.
[34] N. Liu, L. Hu, M.T. McDowell, A. Jackson, Y. Cui, Prelithiated silicon nanowires as an anode for lithium ion batteries, ACS Nano 5 (2011) 6487–6493.
[35] J. Zhao, H.-W. Lee, J. Sun, K. Yan, Y. Liu, W. Liu, Z. Lu, D. Lin, G. Zhou, Y. Cui, Metallurgically lithiated SiOx anode with high capacity and ambient air compatibility, Proc. Natl. Acad. Sci. U.S.A. 113 (2016) 7408–7413.
[36] Q. Meng, G. Li, J. Yue, Q. Xu, Y.-X. Yin, Y.-G. Guo, High-performance lithiated SiO x anode obtained by a controllable and efficient prelithiation strategy, ACS Appl. Mater. Interfaces 11 (2019) 32062–32068.